

OS3-3

高温酸化物融体の構造と物性

Structure and physical properties of high-temperature
oxide melts

Shinji KOHARA¹, Yuta SHUSEKI², Tomoaki KANEKO³, Keitaro SODEYAMA¹, Yohei ONODERA²,
Chihiro KOYAMA⁴, Atsunobu MASUNO², Motoki SHIGA⁵, Junpei T. OKADA⁵, Akitoshi
MIZUNO⁶, Yuki WATANABE⁷, Yui NAKATA⁷, Koji OHARA⁸, Hirohisa ODA⁴ and Takehiko
ISHIKAWA⁴

¹物質・材料研究機構, National Institute for Materials Science,

²京都大学, Kyoto University,

³高度情報科学技術研究機構, Research Organization for Information Science and Technology,

⁴宇宙航空研究開発機構, Japan Aerospace Exploration Agency,

⁵東北大学, Tohoku University,

⁶函館工業高等専門学校, National Institute of Technology, Hakodate College,

⁷エイ・イー・エス, Advanced Engineering Services Co., Ltd.,

⁸島根大学, Shimane University

1. Introduction

Investigation of high-temperature oxide melt is very challenging because chemical reactions with containers are very difficult to avoid. Moreover, the contribution of diffraction from a crystalline container makes it difficult to obtain high-quality diffraction data from high-temperature oxide melts. However, the use of levitation technique¹⁾ can overcome these problems and enable deep undercooling and enhanced glass formation owing to the elimination of extrinsic heterogeneous nucleation. Recently, studies on high-temperature oxide melts and the formation of oxide glasses from supercooled oxide melts using levitation techniques have been of particular interest in understanding the structure of these materials and the process of glass formation. Quantum beam diffraction measurements using synchrotron X-rays and neutrons combined with density measurements at the International Space Station (ISS) are a powerful tool to study the structure and dynamics in high-temperature oxide melts and glasses.

We have been working on high-temperature glass-forming liquid oxides, *e.g.* SiO₂ and non-glass-forming oxide melts, *e.g.* Al₂O₃²⁾ and ZrO₂³⁾ to uncover the relationship between glass-forming ability and atomistic structure of high-temperature oxide melts. We review our previous studies and report recent studies on liquid Er₂O₃ melt⁴⁾ and MgO–SiO₂ melts by density and X-ray diffraction measurements, and reverse Monte Carlo (RMC) – molecular dynamics (MD) simulations.

2. Experimental

2.1 Density measurement

The densities of high-temperature oxide melts were measured with an electrostatic levitation furnace (ELF)⁵⁾ at the ISS. A sample of 2 mm in diameter. It was charged by friction or contact with other materials in ISS–ELF and then levitated to the center between six electrodes that apply Coulomb force. The sample position was stabilized by tuning voltages between electrodes and monitoring the image of the sample backlit by a He–Ne laser. The levitated samples were heated and melted by four 40 W semiconductor lasers. The temperature of the sample was measured by a pyrometer. The sample image was observed by ultraviolet back light and a CCD camera. The sample volume was calculated from its diameter obtained from the image and the density was calculated from the volume and weight of the sample specimen.

2.2 Diffraction measurements

The X-ray diffraction measurements of high-temperature oxide melts were performed at the BL04B2 beamline of SPring-8 using an aerodynamic levitator⁶⁾. The energies of the incident X-rays were 61.4 and 113 keV. The 2-mm sample was levitated in dry air and heated by a 200W CO₂ laser. The temperature of the sample specimen was monitored by a two-color pyrometer. The measured X-ray diffraction data were corrected for polarization, absorption, and background, and the contribution of Compton scattering was subtracted using standard analysis procedures⁶⁾.

The neutron diffraction measurements of high-temperature oxide melts were conducted on the NOMAD diffractometer⁷⁾ at SNS of Oakridge National Laboratory using an aerodynamic levitator. The 3-mm sample was levitated in dry argon and heated by a 400W CO₂ laser. The temperature of the sample specimen was monitored by a two-color pyrometer. The measured scattering intensities for the samples were corrected for instrument background, absorption of the samples, and multiple scattering and incoherent scattering and then normalized by the incident beam profile.

The fully corrected data sets were normalized to give the Faber–Ziman⁸⁾ total structure factor $S(Q)$, and the total correlation function $T(r)$ was obtained by a Fourier transform of $S(Q)$.

2.3 RMC–MD simulation

RMC–MD simulation was performed to determine an atomic configuration of high-temperature oxide melts in a cubic box to reproduce X-ray and/or neutron $S(Q)$. After the MD simulation, RMC refinement was conducted using RMC++ code⁹⁾.

3. Results and discussion

3.1 Density of Er₂O₃ melt

Figure 1 shows the density of Er₂O₃ melt as a function of temperature⁴⁾, which shows a linear temperature dependence. The least-squares fit to the measured data is given by the following equation:

$$\rho(T) = \rho_m [1 - \alpha(T - T_m)](\text{kg/m}^3) \quad (1)$$

where ρ_m is the density at T_m (8170 kg/m³) and α ($=1/\rho_m[d\rho(T)/dT]$) is the thermal expansion coefficient which is assumed to be constant ($1.0 \times 10^{-4} \text{ K}^{-1}$). The uncertainty in the measurements is estimated to be 2%.

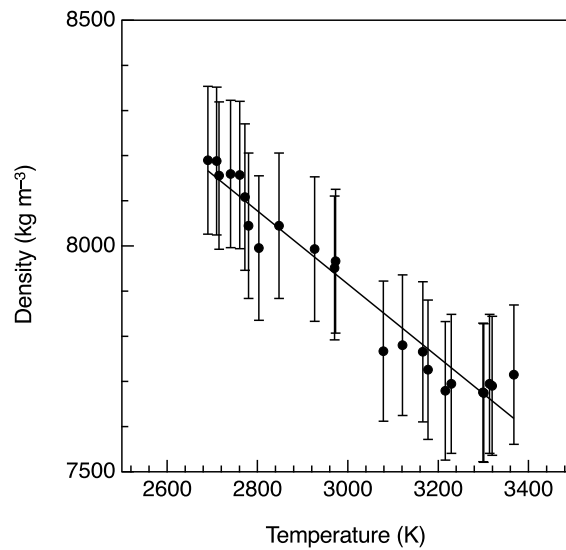


Figure 1. Density of Er₂O₃ melt as a function of temperature⁴⁾.

3.2 X-ray diffraction data of Er₂O₃ melt

The X-ray total structure factors $S(Q)$ of Er₂O₃ melt together with the results of the RMC–MD simulation⁴⁾ are compared in Fig. 2. As can be seen in the figure, the experimental $S(Q)$ data is well reproduced by the RMC–MD simulation. The first peak observed at $Q=2.1 \text{ \AA}^{-1}$ can be assigned to the principal peak whose width is much narrower than those of SiO₂, Al₂O₃ and ZrO₂ melts.

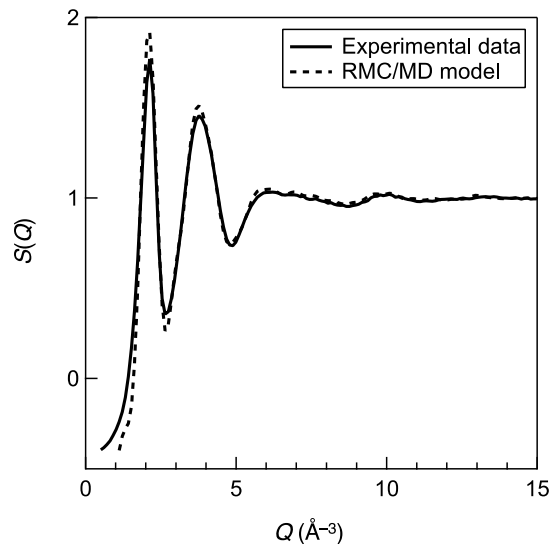


Figure 2. X-ray total structure factors, $S(Q)$ of Er_2O_3 melt at 2923 K⁴.

References

- 1) D. L. Price: High-Temperature Levitated Materials, Cambridge University Press (2010).
- 2) L. B. Skinner, A. C. Barnes, P. S. Salmon, L. Hennem, H. E. Fischer, C. J. Benmore, S. Kohara, J. K. R. Weber, A. Bytchkov, M. C. Wilding, J. B. Parise, T. O. Farmer, I. Pozdnyakova, S. K. Tumber and K. Ohara: Joint diffraction and modeling approach to the structure of liquid alumina. *Phys. Rev. B*, **87** (2013) 024201, DOI: 10.1103/PhysRevB.87.024201.
- 3) S. Kohara, J. Akola, L. Patrikeev, M. Ropo, K. Ohara, M. Itou, A. Fujiwara, J. Yahiro, J. T. Okada, T. Ishikawa, A. Mizuno, A. Masuno, Y. Watanabe and T. Usuki: Atomic and electronic structures of an extremely fragile liquid. *Nat. Commun.*, **5** (2014) 5892, DOI: 10.1038/ncomms6892.
- 4) C. Koyama, S. Tahara, S. Kohara, Y. Onodera, D. R. Småbråten, S. M. Selbach, J. Akola, T. Ishikawa, A. Masuno, A. Mizuno, J. T. Okada, Y. Watanabe, Y. Nakata, K. Ohara, H. Tamaru, H. Oda, I. Obayashi, Y. Hiraoka and O. Sakata: Very sharp diffraction peak in nonglass-forming liquid with the formation of distorted tetraclusters. *NPG Asia Mater.*, **12** (2020) 43, DOI: 10.1038/s41427-020-0220-0.
- 5) H. Tamaru, C. Koyama, H. Saruwatari, Y. Nakamura, T. Ishikawa and T. Takada: Status of the Electrostatic Levitation Furnace (ELF) in the ISS-KIBO. *Microgravity Sci. Technol.*, **30** (2018) 643, DOI: 10.1007/s12217-018-9631-8.
- 6) K. Ohara, Y. Onodera, M. Murakami and S. Kohara: Structure of disordered materials under ambient to extreme conditions revealed by synchrotron x-ray diffraction techniques at SPring-8—recent instrumentation and synergic collaboration with modelling and topological analyses. *J. Phys.: Condens. Matter*, **33** (2021) 383001, DOI: 10.1088/1361-648X/ac0193.
- 7) J. Neuefeind, M. Feygenson, J. Carruth, R. Hoffmann and K. K. Chipley, The nanoscale ordered materials diffractometer NOMAD at the spallation neutron source SNS. *Nucl. Instrum. Meth. B*, **287** (2012) 68, DOI: 10.1016/j.nimb.2012.05.037.
- 8) T. E. Faber and J. M. Ziman: A theory of the electrical properties of liquid metals. *Philos. Mag.*, **11** (1965) 153, DOI: 10.1080/14786436508211931.
- 9) O. Greben, P. Jávári, L. Temleitner and L. Pusztai: A new version of the RMC++ Reverse Monte Carlo programme, aimed at investigating the structure of covalent glasses. *J. Optoelectron. Adv. Mater.*, **9** (2007) 3021.



© 2023 by the authors. Submitted for possible open access publication under the terms and conditions of the Creative Commons Attribution (CC BY) license (<http://creativecommons.org/licenses/by/4.0/>).